High temperature oxidation behaviour of titanium after shot-peening

A. Kanjer [a], V. Optasanu [a], L. Lavisse [a], M.C. Marco de Lucas [a], P. Berger [b], M. François [c] T. Montesin [a]
[a] ICB, UMR 6303 CNRS – Université de Bourgogne Franche-Comté, France, armand.kanjer@u-bourgogne.fr, Virgil.Optasanu@u-bourgogne.fr, Luc.Lavisse@u-bourgogne.fr , Carmen.Marco-de-Lucas@u-bourgogne.fr, Tony.Montesin@u-bourgogne.fr; [b]CEA Saclay, France, Pascal.Berger@cea.fr, [c]Institut Charles Delaunay (ICD)/LASMIS, UMR 6281 CNRS – Université de Technologie de Troyes, France, manuel.francois@utt.fr

Keywords: Titanium, shot-peening treatment, microstructure, oxides and nitrides, surface analysis

Introduction

A wider use of Ti alloys at high operating temperature in gas-turbine engines and other industrial components could be reached by a better protection against high temperature oxidation. The excellent combination of light-weight and good mechanical properties makes the Ti alloys attractive for compressor section components in gas turbine engines[1]. Compared to Ni-super alloys and steels, Titanium offers potential weight savings in the order of 50%. High-performance coatings or surface treatments are necessary for protection against high-temperature oxidation. At low temperatures, Ti alloys show very good corrosion resistance thanks to the TiO_2 passive surface layer. Above 600 °C, a deterioration of the passivation layer and then an acceleration of the oxidation rate is possible. The result is an inward diffusion of oxygen and an internal formation of a rich oxygen-content area, called the α-case[2]. In the case of the oxidation in air, the formation of a nitride layer between the oxide layer and the α-case area was observed[3]. This nitride layer slows down the oxygen diffusion and then brings a protection in terms of oxidation. A problem for the oxidation resistance can be the possible spallation of the oxide film.
The development of efficient oxidation-resistant coatings for titanium alloys is necessary. Two main problems are usually encountered in the high-temperature oxidation of surface treated Ti alloys: (1) interdiffusion between the coating and the bulk and (2) the cracking of the coating or oxide layer. The most usual treatments are ion implantation[4], pack cementation coatings[5] and PVD ceramic coatings[6]. Mechanical treatments are less used for oxidation protection purposes but are widely used to obtain an enhancement of the mechanical surface properties like tribological or fatigue behaviours[7-9]. A recent work[10] shows a positive role of the mechanical treatments in the oxidation resistance of materials after the generation of large compressive stresses on sub-surface.

Objectives

This work investigates the influence of the shot-peening (SP) of commercial pure Titanium on the high-temperature oxidation resistance at 700 °C in dry air and pure oxygen for short oxidation periods (<100 h). The oxidation behavior is studied by thermo-gravimetric analysis (TGA). Subsequently, the surface modifications and the oxide and □-case layers are analysed by X-ray diffraction (phase and residual stresses), optical microscopy, scanning electron microscopy coupled with energy dispersive spectroscopy (SEM/EDS), Raman spectroscopy, microhardness, roughness-measurements and nuclear reaction analysis (NRA).

Methodology

Commercially pure 1 mm-thick Titanium plates (99.8%, Goodfellow) were used in this study. This is a typical grade II material. The material was annealed after processing by the manufacturer in order to annihilate the thermo-mechanical history. The grain size is approximately 35 μm.
The mechanical treatment used in this study is ultrasonic shot-peening. This is a mechanical surface treatment process based on impacting the sample surface with 2mm WC balls. The balls and the sample are placed on a sonotrode, located at the bottom of the treatment chamber that vibrates with a frequency of 20 kHz and projects the balls on the sample surface. The distance between the sonotrode and the sample is 15 mm and the amplitude of vibration is 12 μm. The repetition of the

impacts on the sample generates large residual compressive stresses, plastic deformation within a layer of several hundreds of μm under the surface of the material[11]. For specific conditions, it can also lead to a grain refinement down to a few tens of nanometres. Two treatments with different durations were used here: 10 and 30 minutes per face with face change every 10 minutes. Several parameters as the impact angles, shot velocities and surface coverage, determine the residual stresses profile. For simplicity, further in this text the untreated samples will be called US, the 10 min shot-peened samples will be called SP10 and the 30 min shot-peened samples will be called SP30.

The oxidation experiments were carried out at 700 °C in dry air during 5, 10 and 100 hours. Oxidations kinetic curves were recorded using a thermo gravimetric analyzer SETSYS EVOLUTION 1750 by SETARAM. A ramp of 10 °C/min was used from room temperature to 690 °C, followed by a ramp of 1°C/min to reach 700 °C.

After mechanical treatments and oxidation, X-ray diffraction was used for characterizing the structural phases (D8-A25 DISCOVER, Bruker) with Cu-Kα radiations in the 2θ range of 20 to 100° with an increment of 0.02° and 2s/step.

The residual stresses were investigated by XRD (4 Circles SEIFERT PTS) and incremental electro-polishing (LectroPol-5, STRUERS). The $\sin^2\psi$ method is used for this characterization where ψ is the tilting angle in the range of -60/+60° (χ mode). The X-ray source was Cu-Kα radiation and the peak used was {222} in the 2θ range of 135-145°. The stresses are determined to assume the plane stresses hypothesis ($\sigma_{zz}=0$) and the assumption that $\sigma_{xx} \approx \sigma_{yy}$ where z is the direction normal to the surfac of the sample while x and y are the in-plane directions.

The microstructural characterization of the samples was performed using an optical polarizing microscope (Olympus BX 60) and SEM with BSE (back-scattering electron) mode and EDS analyzer (TESCAN VEGA 3). The morphology and the thickness of the oxide and α-case area were also investigated by SEM. The differentiation between Ti and N is very difficult with EDS because of the close X-Ray emission of the two materials (Kα1=392.4 eV for N and Lα1=452.2 eV for Ti). The problem is solved using NRA-analysis on the cross section. This technique is based on nuclear reaction between light elements and ionized heavy particles (deuterons beam, here)[12]. This technique allows quantifying light elements composition, as N, O, C, F etc. A beam energy of 1.9 MeV is used here to detect $^{14}N(d,\alpha1)^{12}C$ nuclear reaction.

An Invia Renishaw set up in back scattering configuration was used for the acquisition of micro-Raman spectra. The wavelength was 532 nm and the power was about 0.5 mW to avoid heating the samples.

Results and analysis

Results on US (untreated samples) and SP (shot-peened samples) are summarized Fig. 1. Strong modifications are observed under the surface of the treated samples. The optical and SEM micrographs show that the affected thickness by shot-peening treatment is about 130 μm and 190 μm for SP10 and SP30, respectively. Near the surface, the grains of SP10 and SP30 present twinning and smaller grain size than US samples. An increase of Ra and Rt parameters was found after shot-peening treatments (about 75% for Ra and about 50% for Rt).

Microhardness measurements profiles were obtained on cross-section before and after shot-peening. The hardness of pure titanium samples used here is about 135 HV. A strong increase of the hardness (up to 210 HV) near the surface of the shot-peened samples followed by a progressive decrease to the initial value (~ 135 HV) at ~180 μm of the sample surface.

Figure 2 presents in-depth residual stresses profiles on US, SP10 and SP30 samples. The measurements were led up to 200 μm in-depth by incremental electrochemical polishing and XDR analysis. The residual stresses-field profile is characteristic of shot-peening treatments. All samples present compressive residual stress. The untreated material shows compressive-stress smaller than 100 MPa. For SP10 and SP30, the compressive stress goes up to -340 MPa and -330 MPa,

respectively. At 200 µm under the surface, the value of the stress becomes -175 MPa and -220 MPa for SP10 and SP30, respectively.

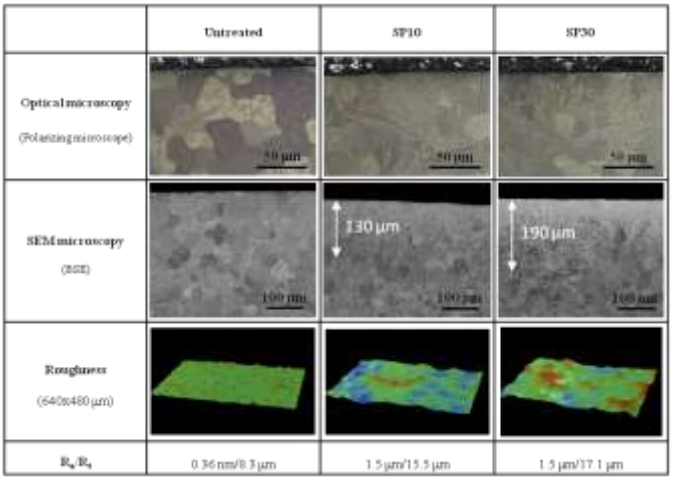

Fig. 1. Comparison between untreated and shot-peened samples.

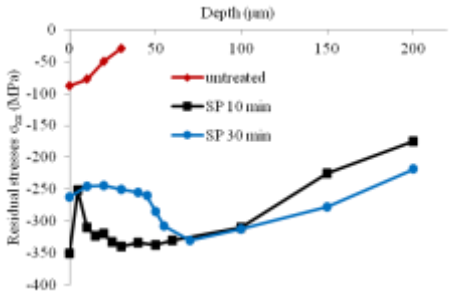

Fig. 2. Residual stress profile of the samples.

The shot-peening treatment deforms and disturbs only the extreme surface of the samples. The intensity of the microstructural modifications decreases with the depth. One can notice a gradient of twinning density and grains refinement from the surface to the bulk of the sample. Hardness measurements show gradients of work hardening and strong plastic strains in the SP10 and SP30 sub-surface. For SP10 and SP30, the residual stresses profiles have typically two parts: accommodation and adaptation zones. The accommodation zone is near the surface and presents high stress-level. The adaptation zone corresponds to the stress gradient region. SP30 accommodation area seems to be shifted and broadened in comparison with SP10 (see Fig. 2). Furthermore, the highest absolute value of the compressive stress is higher for SP10 than for SP30. The residual stress is mainly produced by the gradient of the plastic deformation. It is possible that for, SP30, the repetition of impacts on the surface leads to a partial relaxation of the compressive residual stresses, by imposing a quasi-constant plateau. By contrast, the residual stresses profile for SP30 became stronger than for SP10 after about 100 µm depth.

Several authors[14,15] also reported grains refinement, hardness increase and generation of residual stresses after ultrasonic shot-peening treatment. Generally, these observations depend on the treatment parameters as the processing time, the surface coverage or the sonotrode vibration frequency. The mechanism of titanium deformation during the treatment, proposed in literature[16], consists of an activation of slip planes and a twinning of grains followed by grain refinement.

XRD and Raman analyses are presented in Fig. 3a and 3b, respectively. The main phase detected by XRD is titanium-α. A broadening of the peaks is obtained for the SP samples: this comes from crystallites size reduction and crystal lattice distortion due to an increase in dislocation density. Pollution after shot-peening on SP30 sample surface is confirmed. For SP30, a second phase was detected: tungsten carbide, coming from the wear of WC balls on the sample surface. One can also note a partial change in the crystallographic texture of the surface shown by the lower relative intensity of the peak at 70° (Fig. 3a).

Figure 3b presents Raman spectroscopy of US and SP samples before oxidation. For the untreated sample no phase was detected (the α-Ti phase cannot be seen by this technique). On the other hand, for SP10 and SP30 respectively the first set of large Raman bands (210 cm^{-1} and 640 cm^{-1}) correspond to a non-stoichiometric titanium oxide or oxynitride (TiO_xN_y)[17]. During SP treatment, oxidation and nitriding induce the formation of Ti(N,O) phases. A second set of Raman bands were

detected between 1350 cm^{-1} and 1600 cm^{-1} and correspond to carbon-carbon vibrational modes (D and G modes, respectively)[18]. This pollution of the sample surface can also be explained by the SP treatment with WC balls.

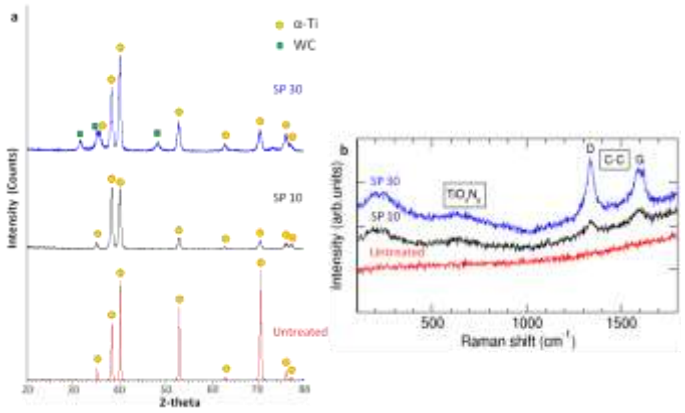

Fig. 3. XRD and Raman results before oxidation

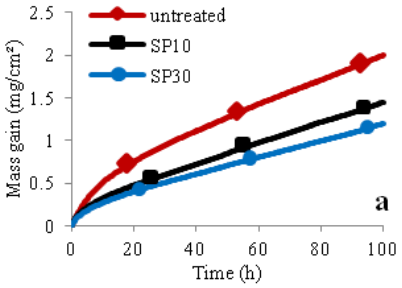

Fig. 4. TGA curves

Figure 4 presents different oxidation kinetic curves for 100 hours at 700 °C under dry air. Under dry air, SP treatments lead to a smaller mass gain. A mass gain reduction of about 30% and 45% is observed for SP10 and SP30, respectively. The good behavior of the shot-peened samples to the high temperature oxidation is influenced by the mechanical state of the matter, even if at those temperatures a recrystallization occurs rapidly.

Different phases were detected by XRD after oxidation in dry air at 700 °C after 5 h, 10 h and 100 h of oxidation. After 5 h and 10 h of oxidation, rutile and anatase phases were detected on both SP10 and SP30. Nitrides like Ti_2N and $TiN_{0.176}$ were detected after 5 h and 10 h of oxidation. WO_3 was also found for short-time oxidations of SP30 samples. The rutile phase is the main phase formed after 100 h of oxidation but the anatase phase is also detected for SP30.

Figure 5 displays a superposition of Raman spectroscopy analyses for US, SP10 and SP30 after 5 h of oxidation. For US sample, only TiO_2 in the rutile (R) phase was found. For SP10 and SP30 samples, TiO_2 crystallized in both the anatase (A) and the rutile (R) phases. Moreover, as a function of the analyzed area, different Raman spectra were found for SP30. Figure 5 presents two of those spectra called here SP30(1) and SP30(2). The very strong Raman peaks of SP30(2), located at 750 cm^{-1} and 850 cm^{-1} are characteristic of the hexagonal WO_3 phase[19]. This result shows that WC fragments transferred from the SP balls to the sample surface, revealed by XRD patterns (Fig. 3a), are oxidized with the oxidation conditions used here. The other spectrum, SP30 (1) is similar to those obtained for SP10 and US samples. So, a heterogeneous distribution of WO_3 grains is found on the surface of SP30 samples after oxidation at 700 °C.

WC pollution seems to cause the WO_3 oxide formation. This is confirmed by XRD and Raman spectroscopy analyses. Kumar et al.[20] work on titanium oxidation confirm the presence of rutile on the sample surface after oxidation. Guleryuz et al.[21] found anatase on TA6V samples oxidized during 48 h at 650 °C, but not on samples oxidized at 700 and 750 °C. The refinement of microstructure seems to play an important role in the anatase formation at early stages of the oxidation.

Figure 6 presents the microstructural and morphological characterization of oxidized samples on the cross-section, after mounting in resin and polishing. US oxide-scale thickness is about 11 µm thick (after 100 h of oxidation at 700 °C under dry air). The SP10 and SP30 oxide thickness are about 7 µm and 5 µm, respectively. The adherence seems to be more important for US samples. All samples presented stratification and internal porosities after oxidation. The stratification for pure titanium was also reported by several authors[20,21]. In-depth insertion of oxygen is disturbed by the mechanical treatment. Indeed, the thickness of the α-case zone, determined by micro-hardness

measurements, is about 5 µm and 10 µm larger for SP10 and respectively for SP30 compared to untreated samples. This can be explained by the increasing of the reactivity of the surface given by the mechanical modifications due to the shot-peening. Gutman et al.[22] worked on the impact of mechanical treatments on the chemical-thermodynamics parameters and showed that stresses and plastic strains induced by SP lead to an acceleration of surface reaction and an increase of the entropy. Hence, the diffusion of oxygen and nitrogen into the oxide scale enhances the formation of rutile and nitride. Wen et al.[23] have observed, after SMAT treatment and oxidation for 1 h at 700 °C on pure Ti, an increase of oxygen, nitrogen and carbon contents on the surface.

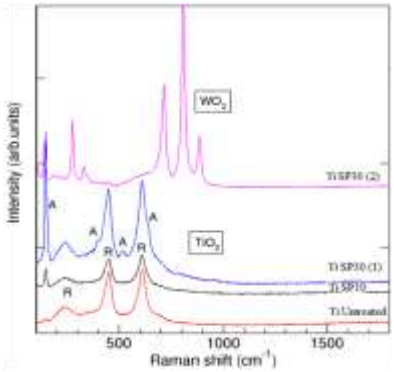

Fig. 5. Raman spectra.

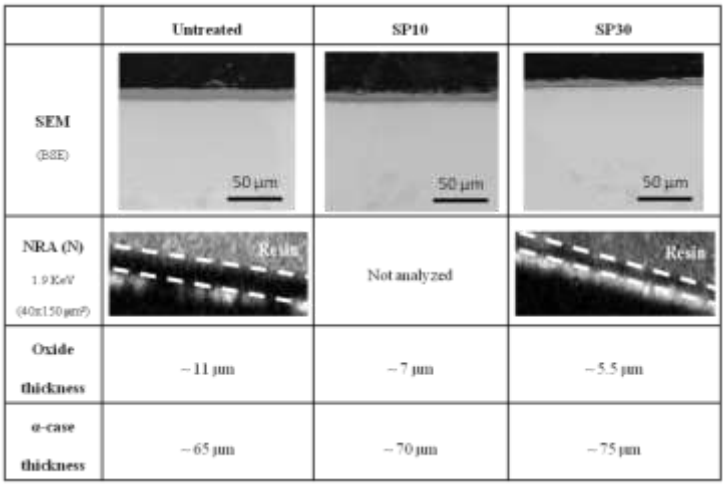

Fig. 6. Morphology of the samples cross-section

The determination of nitrogen distribution was made by NRA analysis. The particular conditions used here allow visualizing only the zones of the sample where nitrogen is present. For the NRA maps, the coating resin is located in the upper part while the alpha-case area is positioned at the bottom of the picture. The oxide is localized between the dashed white lines. The detection of nitrogen in the resin part was explained by its composition (nitride aromatic heterocycles). This analysis shows nitrogen-rich area on samples cross section localized between the oxide layer and the α-case area (bright thin stratum under the oxide layer in Fig. 6). It is important to notice the discontinuity of the rich nitride area for untreated samples. In contrast, the nitride layer for SP samples is continuous and can form a barrier against the oxygen diffusion. This confirmed the high importance of the nitrogen in the high-temperature oxidation mechanism of titanium under air[4].

One can propose the following mechanism for the high-temperature oxidation of shot-peened samples: The shot-peening treatment introduces a high density of dislocations and intense grain refinement (Fig. 1). This locally increases the apparent diffusion coefficient of light elements such as O and N. This is confirmed by the larger α-case area measured by micro-hardness on shot-peened samples. Light elements (O, N) can diffuse through the oxidation surface layer. Coddet et al.[4] remarked that the nitrogen diffusion coefficient through the oxide layer is larger than for the oxygen. In contrast, nitrogen diffuses in pure Ti ten times less than oxygen[4]. Defects allow O to diffuse more easily in the cold-worked metal, producing then an accumulation of nitrogen at the interface oxide/metal, as proved by the XRD analysis and NRA measurements (Fig. 6). Thus, before defects recovery, nitrides can be formed at the interface and produce a barrier for the oxygen. The flux of oxygen into the metal becomes lower for shot-peened samples, which explains their thin oxide scale. The nitrides can also play a role in the accommodation between the metal and the oxide scale, giving then a better adherence and less spallation of the oxide in the shot-peened samples case. The nature of the oxide can also be different for shot-peened samples and can explain the differences in oxidation behaviours (anatase is detected by XRD and Raman in SP30 samples: Fig. 5).

This formation and the increasing of roughness parameters after treatments (Fig. 1) can also play a role in the adherence of oxide scale.

Conclusions

The impact of a surface mechanical treatment by ultrasonic shot-peening on the oxidation kinetics of pure titanium at 700 °C during 100 h under dry air or pure oxygen has been studied here. The influence of the SP treatment duration (10-30 minutes) has also been studied.

Shot-peened samples present a higher oxidation resistance (about 30 to 45% of mass gain reduction by comparison with US). The main phases formed after oxidation are rutile and anatase. For short oxidation time, nitride and WO_3 phases are detected. By consequence, the surface contamination by the WC balls is noticed and can play a role in the mass gain reduction. The formation of anatase can explain the oxide layer brittleness. NRA analysis shows, in SP samples, the formation of a continuous nitride layer between the oxide layer and α-case area. During the first stages of oxidation, before the defects recovering, the increase of the surface entropy, the grains refinement and the twinning increase the inward diffusion of oxygen and nitrogen.

Two causes can be proposed to explain the mass grain reduction after oxidation: (1) a microstructural modification and a mechanical effect after treatments due to the twinning and grains refinement, (2) a chemical effect with rapid formation of a nitride continuous layer between the oxide and the α-case area.

References

[1] J.C. William and E.A. Starke, Acta Materialia, 2003, **51,** 5775-5799.
[2] J. Stringer, Acta Metallurgica, 1960, **8**, 758-766.
[3] A.M. Chaze and C. Coddet, Journal of the Less Common Metal, 1986, **124**, 73-84.
[4] I. Gurappa, D. Manova, J.W. Gerlach, S. Mandl and B. Raushenbach, Surface and Coating Technology, 2006, **201**, 3536-3546.
[5] D.K. Das and S.P. Trivedi, Material and Surface Technology, 2004, **367**, 225-233.
[6] A. Ebach-Stahl, C. Eilers and N. Laska, Surface and Coating Technology, 2013, **223**, 24-31.
[7] Y. Fu, N.L. Loh, A.W. Batchelor, D. Liu, X. Zhu, J. He and K. Xu, Surface and Coatings Technology, 1998, **106**, 193-197.
[8] L. Wagner and G. Lutjering, International Conference on Shot-Peening, 1996.
[9] X. P. Jiang, C.S. Man, M.J. Shepard and T. Zhai, Materials Sciences and Engineering: A, 2007, **468-470**, 137-143.
[10] L. Raceanu, V. Optasanu, T. Montesin, G. Montay and M. François, Oxidation of Metal, 2013, **79**, 135-145.
[11] M. Micoulaut, S. Mechkov, D. Retraint, P. Viot and M. François, Granular Matter, 2005, **9**, 25-33.
[12] H. Khodja, E. Berthoumieux, L. Daudin and J.P. Gallien, Nuclear Instruments and Methods in Physics Research Section B: Beam Interaction with Materials and Atoms, 2001, **181**, 83-86.
[13] A. Gurbich and S. Molodtsov, Nuclear Instruments and Methods in Physics Research Section B: Beam Interaction with Materials and Atoms, 2008, **266**, 1206-1208.
[14] S.B. Fard and M. Guagliano, Frattura e Integrita Strutturale, 2009, **7,** 3-16.
[15] M. Thomas and M. Jackson, Scripta Materialia, 2012, **66**, 1065-1068.
[16] K.Y. Zhu, F. Vassel, K. Ju and J. Lu, Acta Materialia, 2004, **52**, 4101-4110.
[17] L. Lavisse, P. Berger, P.M. Cirisan, J.M. Jouvard, S. Bourgeois and M.C. Marco de Lucas, Journal of Physic D: Applied Physics, 2009, **42**, 245-303.
[18] J.M. Chappé, M.C. Marco de Lucas, L. Cunha, C. Moura, J.F. Pierson, L. Imhoff, O. Heintz, V. Potin, S. Bourgeois and F. Vaz, Thin Solid Films, 2011, **520**, 144-151.
[19] M. Boulova and G. Lucazeau, Journal of Solid State Chemistry, 2002, **167**, 425-434.
[20] S. Kumar, T.S.N.S. Narayanan, S.G.S. Raman and S.K. Seshadri, Materials Characterization, 2010, **61**, 589-597.
[21] H. Guleryuz and H. Cimenoglu, Journal of Alloys and Compounds, 2009, **472**, 241-246.
[22] E.M. Gutman, 22-23, 1994, Ed. World Scientific.
[23] M. Wen, C. Wen, P. Hogdson, and P. Li, Colloids and Surface B: Biointerfaces, 2014, **116**, 658-655.